1 September 2000

ELSEVIER

Chemical Physics Letters 327 (2000) 61–68

CHEMICAL PHYSICS LETTERS

www.elsevier.nl/locate/cplett

Inelastic, quasi-elastic and charge transfer scattering in $C_{60}^{+} + C_{60}$ collisions

A.V. Glotov, E.E.B. Campbell *

School of Physics and Engineering Physics, Göteborg University and Chalmers University of Technology, SE-412 96 Göteborg, Sweden

Received 8 May 2000; in final form 14 July 2000

Abstract

Differential cross-section data is presented for quasi-elastically scattered fullerene projectile ions in fullerene-fullerene collisions. The degree of inelasticity is reported as a function of collision energy and scattering angle. In addition, differential cross-section data are reported for resonant charge transfer. The data are used to correct previously reported total cross-section measurements for charge transfer that underestimated the loss of signal due to scattering. © 2000 Elsevier Science B.V. All rights reserved.

1. Introduction

In recent years, there has been increasing interest in the study of collisional interactions between atomic clusters. Collisions between fullerenes are the most studied systems [1,2] and have been shown to be very convenient model systems for such research. Experimental investigations of cluster–cluster collisions with fullerenes have included studies on molecular fusion and fragmentation at intermediate collision energies [3,4] and fragmentation at high collision energies [5]. In addition, charge transfer (CT) at collision energies ranging from thermal to 100 keV has been the subject of a number of investigations using both singly [6] and multiply charged [5,7–9] projectile ions.

We have recently begun a series of experiments at intermediate collision energies (100–1500 eV in the centre-of-mass frame of reference) where we investigate for the first time the scattering angle dependence of the various reaction channels open at these collision energies. In a recent publication, we have reported on the scattering angle dependence of fusion and fragmentation reaction channels [4]. The results were shown to be in very good agreement with simple phenomenological models. The angular and energy dependence of the mass spectra were consistent with a highly statistical behaviour providing additional support for the interpretation of the change in fragmentation behaviour with increasing collision energy in terms of a phase transition [10] for both the products of fusion and inelastically scattered projectile ions. In this Letter, we continue our studies of the angular dependence of possible reaction channels. Here, we focus on the scattering of projectile ions that do not undergo fragmentation on the microsecond timescale of our experiment. We report the angular dependence and inelasticity of the

* Correponding author. Fax: +46-31-772-3496; e-mail: eleanor.campbell@fy.chalmers.se

PII: S0009-2614(00)00853-8

collision as a function of collision energy and compare with the classical differential cross-section for elastic scattering calculated using the Girifalco potential [11,12]. In addition, we look at the competing channel of resonant charge transfer and make some correction to the previously reported total cross-section values that were underestimated due to the effect of scattering outside the small angular detection range in the original experiments [6].

2. Experimental set-up

The experimental set-up is very similar to that described in detail elsewhere [4] and will only be briefly described here with emphasis on the differences compared to the earlier report. A pulsed beam of projectile ions, C_{60}^{+}, produced by energetic electron impact (250 eV), is accelerated to the desired collision energy and focused into a scattering cell. The internal energy of the projectile ions at the collision cell has been estimated, by considering metastable fragmentation, to be approximately 20 eV. The scattering cell contains high purity C_{60} heated to a temperature of 450–500°C. Single-collision conditions are ensured by checking the intensity of the collision products as a function of scattering cell temperature. Projectile and product ions are detected by a rotatable time-of-flight (TOF) mass spectrometer coupled to a multi-channel plate detector and digital multi-channel scalar for single-ion counting. In contrast to the earlier report [4], a linear TOF mass spectrometer is used in the present experiments rather than a reflectron. This also allows the detection of neutral species, in particular the products of resonant charge transfer. A retarding field energy analyser placed before the channel plate detector can be used to determine the kinetic energies of positively charged products as well as to remove all positively charged ions prior to detection when charge transfer is the channel of interest. Such a set-up, without the possibility of rotation, was used in our earlier report of charge transfer involving singly charged fullerene ions [6]. Details of the experimental procedure and data analysis can be found in that paper.

The angular resolution of the experiments in the small scattering angle range of interest is dominated by the angular spread of the projectile ion beam. This was measured to be $\pm 1°$. The energy spread of the projectile ion beam was determined for each set of measurements using the retarding field analyser and was found to be on the order of 5% of the laboratory collision energy.

In the following, all collision energies will be given in the centre-of-mass frame unless otherwise stated.

3. Results and discussion

From the TOF data, we can extract the intensity of the scattered but non-fragmented projectile ions. As was discussed in an earlier paper [4] the scattered, but non-fragmented ions have an angular distribution intermediate between that of the projectile ion beam and the charged fragments. These are ions that may have been scattered elastically or inelastically. If the latter, they have not received sufficient internal excitation energy during the collision to undergo fragmentation on the microsecond timescale of the experiments. A measure of the degree of inelasticity in the collisions can be obtained from measurements of the ion kinetic energies using the retarding field energy analyser. For a scattering angle of 0° the scattering is seen to be very close to elastic. As the scattering angle increases the velocity of the elastically scattered molecules decreases and the maximum in the velocity (or energy) distribution moves in any case towards smaller values. The experiments, however, clearly show that the inelasticity of the collision increases for ions scattered to larger angles, i.e. those ions that have undergone lower impact parameter collisions. The kinetic energy determined by the retarding field analyser shifts significantly to values lower than that for elastic scattering as θ increases.

The classical deflection function for $C_{60}^{+} + C_{60}$ collisions can be calculated from the expression [13]

$$\chi(E,b) = \pi - 2b\int_{r_0}^{\infty}\left(1 - \frac{U(r)}{E} - \frac{b^2}{r^2}\right)\frac{\mathrm{d}r}{r^2} \qquad (1)$$

where χ is the scattering angle in the centre of mass frame, b is the impact parameter, $U(r)$ the intermolecular potential, E the collision energy, r the

intermolecular separation and r_0 the turning point of the collision. As $U(r)$, we use the potential given by Girifalco [11,12] with an additional polarisability term ($-\alpha e^2/r^4$, $\alpha = 80$ Å^3) [14] since we are dealing with ion-neutral collisions. The potential is plotted in Fig. 1 along with the deflection functions calculated for a range of collision energies. This allows us to relate the measured scattering angle to an impact parameter. Due to the rather unusual properties of the intermolecular potential it is not possible to use the normal small angle scattering relationship between $E\chi$ and b. The deflection function has to be calculated for each collision energy. At the rather high collision energies of interest here there is very little influence of the shallow potential well and the interaction probed in the collisions is purely repulsive. The potential rises very rapidly as the cages approach each other and is quite close to a hard sphere potential.

The experimentally determined inelasticities measured for the scattered but not fragmented projectile ions are plotted as a function of both centre of mass scattering angle and impact parameter for different collision energies in Fig. 2. The relative inelasticity (the amount of energy transferred divided by the collision energy in the laboratory frame of reference) is very low up to a scattering angle of about $\chi = 7°$. It then increases roughly linearly with increasing scattering angle. The plot of ΔE versus b shows a slightly higher than linear dependence as the impact parameter decreases. Interestingly, the total amount of energy transferred, rather than the relative amount, scales with b but is practically independent of the collision energy in the range investigated (Fig. 2b). The amount of energy transferred to internal degrees of freedom is such that significant fragmentation can only be expected at the largest scattering angles measured for energies beyond ca. 1000 eV. The ΔE that we give is the total amount of energy transferred to internal degrees of freedom. This will be divided between projectile and target. In order to observe substantial fragmentation, we would need to transfer ca. 20 eV to the projectile vibrational modes. Assuming the internal excitation energy is divided equally between projectile and target this requires the conversion of 40 eV (2% of 1 keV centre-of-mass energy, i.e. 2 keV laboratory energy). The findings can be compared with our earlier report on fragmentation as a function of collision energy and scattering angle. The fragment angular distributions are centred

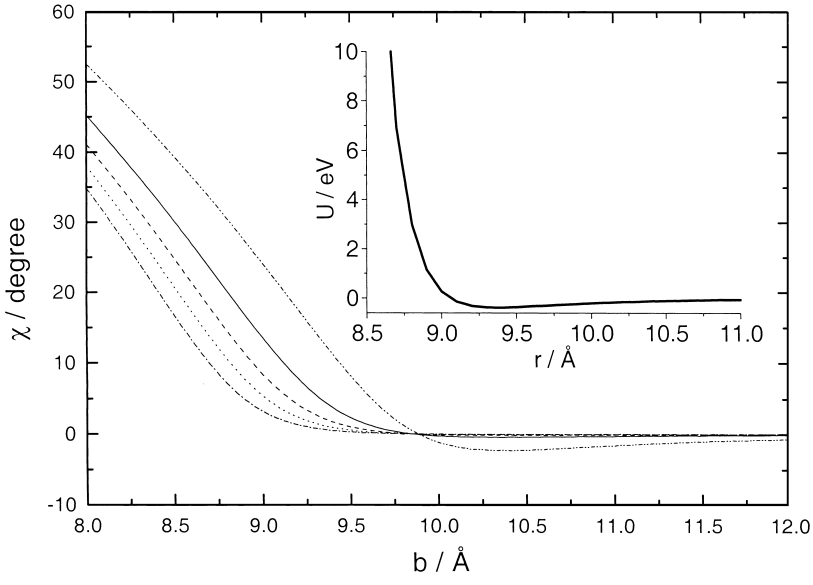

Fig. 1. Calculated classical deflection functions from the Girifalco intermolecular potential including a polarization term, shown in insert (see text). Dashed double-dot: 20 eV; full line: 100 eV; dashed: 250 eV; dotted: 500 eV; and dashed–dot: 1000 eV. All energies given in the centre-of-mass frame of reference.

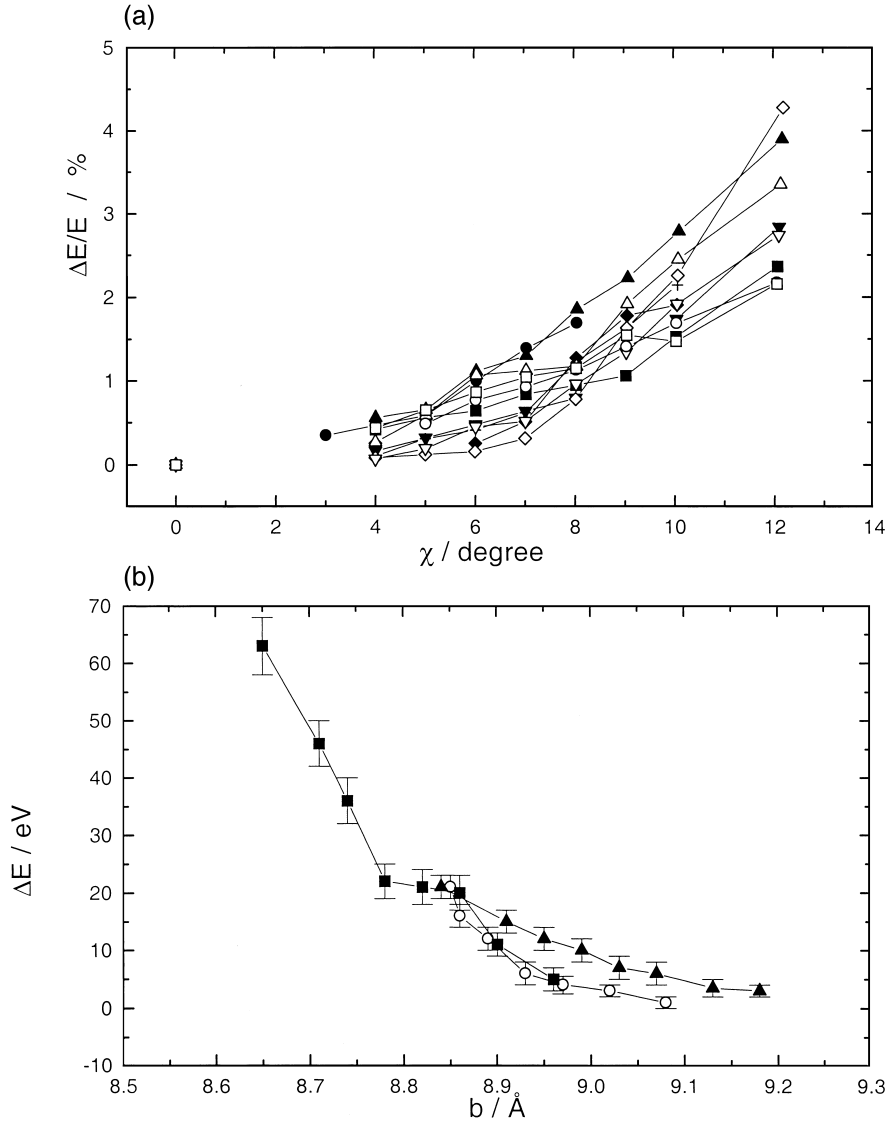

Fig. 2. (a) Relative inelasticity ($\Delta E/E_{\mathrm{Lab}} = 0.5\ (\Delta E/E_{\mathrm{CM}})$) as a function of centre-of-mass scattering angle for the following centre of mass collision energies. ■: 180 eV; ●: 216 eV; ▲: 270 eV; ▼: 318 eV; ◆: 395 eV; □: 490 eV; ◦: 640 eV; △: 785 eV; ▽: 940 eV; ◇: 1445 eV; *: 1390 eV. (b) Absolute inelasticity ΔE plotted as a function of impact parameter for 270 eV (▲); 490 eV (◦); and 940 eV (■).

around centre-of-mass scattering angles of 10–20° depending on collision energy and show a fairly constant relative inelasticity of 30%. A conversion to impact parameter using the Girifalco elastic deflection function would certainly not be expected to be relevant in this case since a very large amount of energy is transferred to internal degrees of freedom with a substantial deformation of the cage during the collision. The Girifalco potential treats the colliding fullerenes as structureless quasi-atoms and can therefore not be expected to give reasonable results when strong deformation is present. The fairly low scattering angles of the fragments should therefore not be related to the rather high impact parameters of around 8.5 Å that would be obtained from simply considering the elastic deflection function, although an ex-

trapolation of the data in Fig. 2b would give internal energies in the correct range.

We can compare the experimental scattering cross-sections determined for the non-fragmented projectile ions with the classical elastic scattering cross-section

$$\sigma(|\chi|,E) = \frac{b}{\sin|\chi| \times |\mathrm{d}\chi/\mathrm{d}b|}. \qquad (2)$$

It is experimentally very difficult to determine absolute cross-sections and the experimental data shown in Fig. 4 have been normalised to the calculated cross-section at a scattering angle of 4°. The relative values are, however, much more accurate and the trend in the experimental cross-sections can be compared to the trend in the calculated classical elastic cross-section. The calculated cross-section is practically independent of collision energy in the range of relevance for our experiments, showing again the closeness to a hard-sphere type behaviour. It is obvious that the scattering becomes more and more quasi-elastic as the collision energy is decreased and the experimental data follows a trend that becomes closer to the calculated one. The principle reason for the strong decrease in the experimental cross-sections at high collision energies and angles is of course the very significant contribution of the fragmentation reaction channel that has not been included in the analysis of the experimental data. This has been discussed at length previously [4].

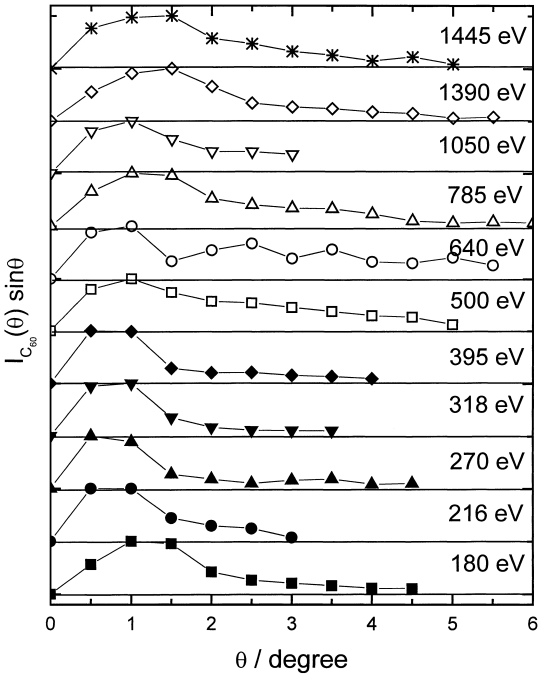

Fig. 3. Intensity as a function of lab. scattering angle for the given collision energies.

There are two further reaction channels at the energies used in the experiments, fusion and resonant charge transfer, that have not yet been considered. The fusion cross-sections are 1–2 orders of magnitude lower than the scattering and CT cross-sections [3,6] and will not be further discussed here. By using a high retarding field before the ion detector, we can remove all positive ion projectiles and collision products and detect only fast neutral products. This method has been used previously to determine CT cross-sections but with a very narrow detection range of $0 \pm 0.6°$. The angular distributions shown in Fig. 3 are for neutral particles that have been scattered elastically and quasi-elastically. In order to obtain this data, a time window for the detection of the products was set in the TOF spectra corresponding to velocities of C_{60} around the velocity expected for elastic scattering. Our previous measurements have shown that the CT peak in the TOF spectra appears where one would expect it assuming no significant transfer of energy to internal degrees of freedom due to the collision [6]. The differential CT cross-section for an energy of 165 eV has been plotted on Fig. 4b for comparison with the scattering cross-sections. Again, the absolute values are very uncertain with the additional uncertainty in the detection efficiency for the neutral fullerenes at the channel plate detector. We have used the same normalisation factor as for Fig. 4a. The data plotted in the figure have been obtained by assuming that the detection efficiency for the neutral fullerene is the same as for a singly charged fullerene at the same impact velocity [6]. The CT cross-section behaves very similarly to the cross-section for scattering of projectile ions but is somewhat smaller. The overall trend is unaffected but the absolute values are shifted upwards when the CT channel is taken into account.

It is clear from Fig. 3 that scattering occurs to angles larger than the detection limit in the original CT experiments and that our original report of the

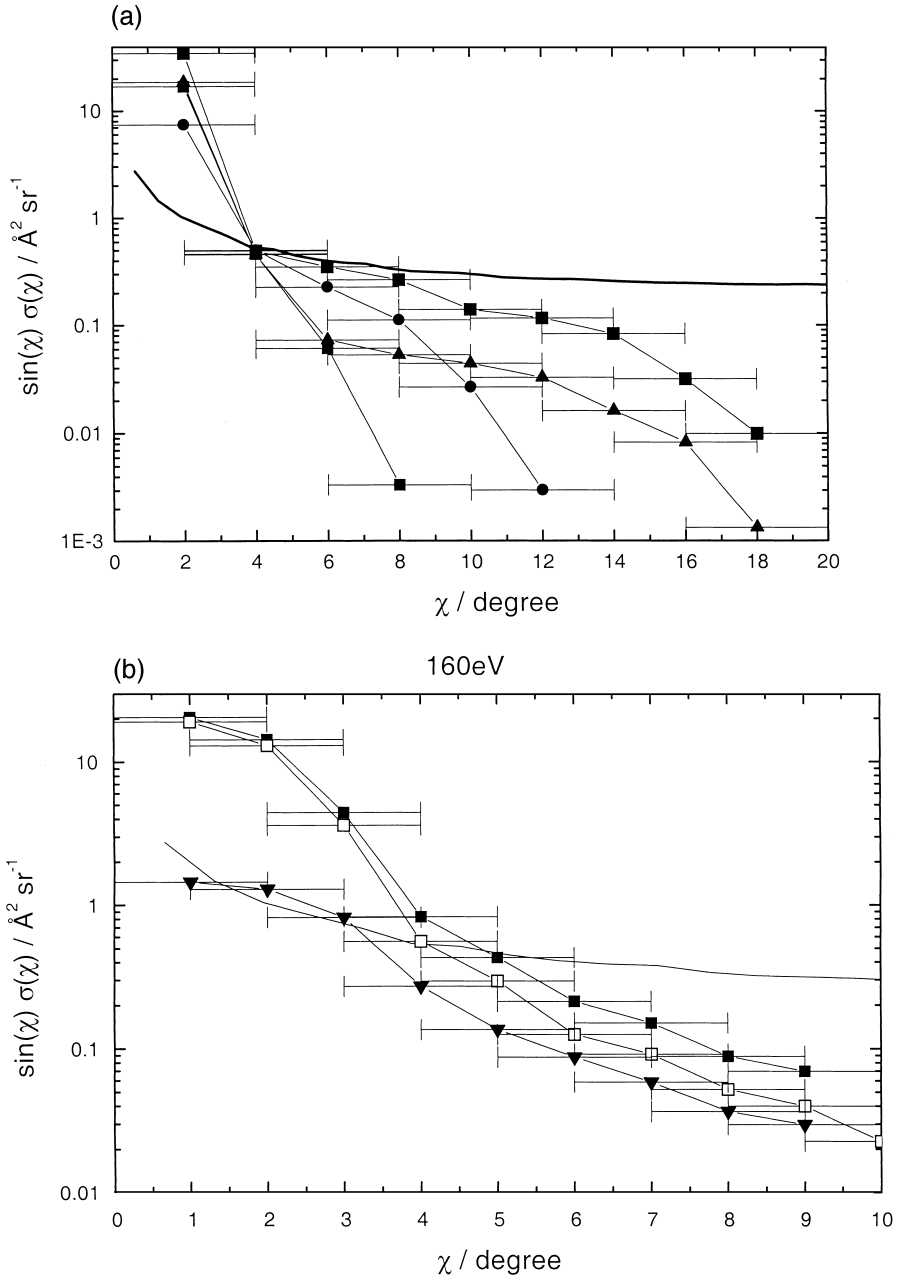

Fig. 4. (a) Comparison of experimentally determined differential scattering cross-sections with the classical elastic scattering differential cross-section. ■: 1380 eV; ●: 500 eV; ▼: 165 eV; □: 131 eV. (b) As (a) for 165 eV but including the experimental CT cross-section (▼).

total CT cross-section thus underestimated the value. The tails on the distributions towards large scattering angles, in particular for collision energies beyond 500 eV, are most likely due to some contribution from small neutral fragments that have been included in our detection window. This is most apparent for the intermediate energies around 500–800 eV where the fragments have a broad angular distribution [4]

and will have significant intensities in the angular range studied in the CT experiments. An analysis of the scattering data allows us to correct the cross-section values reported previously [5]. A comparison of the present correction with the original data is shown in Fig. 5. The overall value has increased by about a factor of two with a larger increase at small collision energies where the loss due to scattering is more significant. The correction brings the data into excellent agreement with the simple two-state model for charge transfer developed for ion–atom collisions by Rapp and Francis [15,16].

As mentioned above, there is considerable uncertainty in the absolute values of the cross-sections determined in the experiment which means that the very good agreement with the simple CT model could be coincidence. The present data has been treated in the same way as in the previous papers for consistency [3,6–8]. The fullerene target density was calculated using the vapour pressure curves given by Abrefah et al. [17], determined by weight loss measurements. More recent reports have suggested that the vapour pressure should be considerably higher [18–20]. The most recent experiments report vapour pressures of nearly an order of magnitude higher than the Abrefah values for the temperature range of interest [20]. This would imply that the collision cross-sections reported by us as well as by other groups [5] should be roughly an order of magnitude smaller. This would give unreasonably small values (much less than the geometrical cross-sections) for the scattering and CT cross-sections. We are thus drawn to the conclusion that the Abrefah vapour pressure values are the most appropriate for our experiment. If the more recent values are in fact correct under our experimental conditions, then some explanation will have to be found for the unexpectedly low absolute cross-sections. A careful measurement of the vapour pressure in our apparatus as carried out by Jaensch and Kamke is unfortunately not possible [20].

In conclusion, we have reported the first differential scattering measurements for elastic and inelastic scattering as well as resonant charge transfer of fullerene projectile ions in collisions with neutral fullerenes. The scattering behaviour is rather unusual due to the very strongly repulsive nature of the intermolecular potential. The degree of inelasticity of the quasi-elastically scattered projectile ions is seen to increase with collision energy and scattering angle. The cross-section for charge transfer behaves similarly to the elastic scattering cross-section. The

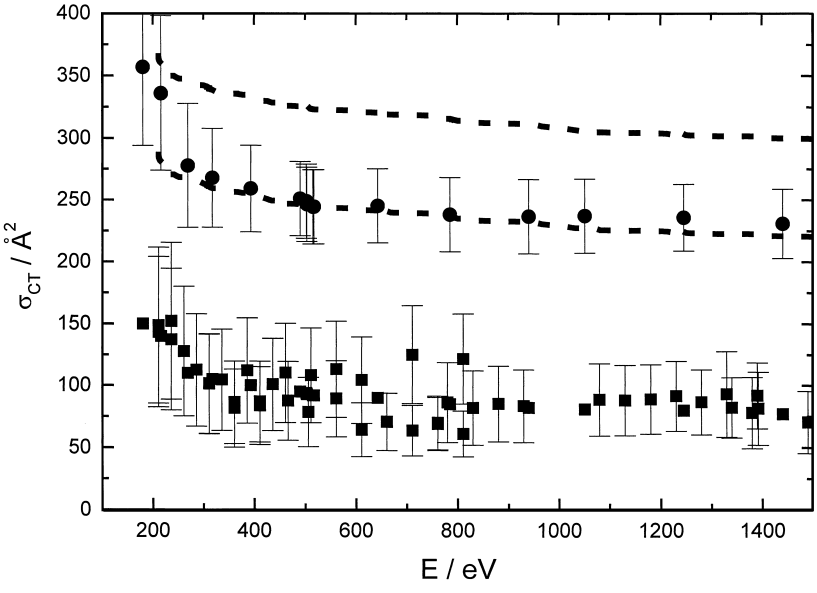

Fig. 5. Total CT cross-section. ■: data published previously [6]. Dotted lines: upper and lower limits estimated from the Rapp and Francis model. Model calculations from Ref. [6]. ●: data corrected for scattering effects using present differential cross-section data.

absolute cross-section values reported previously have been corrected taking loss due to scattering into account. Differential scattering measurements at lower energies (< 100 eV) using a crossed beam set-up rather than a scattering cell would be able to provide a good test of the Girifalco potential. This is presently beyond the possibilities of our apparatus but should not be too difficult to achieve.

Acknowledgements

Financial support by the Swedish Natural Science Research Council (NFR) is gratefully acknowledged.

References

[1] E.E.B. Campbell, F. Rohmund, Rep. Prog. Phys. 63 (2000) 1061.
[2] O. Knospe, R. Schmidt, in: J. Jellinek (Ed.), Theory of Atomic and Molecular Clusters, Springer, Berlin, 1997.
[3] F. Rohmund, A. Glotov, K. Hansen, E.E.B. Campbell, J. Phys. B 29 (1996) 5143.
[4] A. Glotov, E.E.B. Campbell, Phys. Rev. A, in press, 2000.
[5] H. Shen, P. Hvelplund, D. Mathur, A. Barany, H. Cederquist, N. Selberg, Phys. Rev. A 52 (1995) 3847.
[6] F. Rohmund, E.E.B. Campbell, J. Phys. B 29 (1997) 5143.
[7] F. Rohmund, E.E.B. Campbell, Chem. Phys. Lett. 245 (1995) 237.
[8] F. Rohmund, E.E.B. Campbell, Z. Phys. D 40 (1997) 399.
[9] D.K. Bohme, Int. Rev. Phys. Chem. 13 (1994) 163.
[10] E.E.B. Campbell, T. Raz, R.D. Levine, Chem. Phys. Lett. 253 (1996) 261.
[11] L.A. Girifalco, J. Chem. Phys. 96 (1992) 858.
[12] L.A. Girifalco, J. Chem. Phys. 95 (1991) 5370.
[13] R.D. Levine, R.B. Bernstein, Molecular Reaction Dynamics and Chemical Reactivity, Oxford University Press, Oxford, 1987.
[14] A.A. Quong, M.R. Perdersen, Phys. Rev. B 46 (1992) 12906.
[15] D. Rapp, W.E. Francis, J. Chem. Phys. 37 (1962) 2631.
[16] D.P. Dewangen, J. Phys. B 6 (1973) L20.
[17] J. Abrefah, D.R. Olander, M. Balooch, W.J. Siekhaus, Appl. Phys. Lett. 60 (1992) 1313.
[18] V. Piacente, G. Gigli, P. Scardala, A. Gustini, D. Ferro, J. Phys. Chem. 99 (1995) 14052.
[19] P.F. Coheur, M. Carleer, R. Colin, J. Phys. B 29 (1996) 4987.
[20] R. Jaensch, W. Kamke, Mol. Mater., in press, 2000.